The Anti-Tumor Agent, Dp44mT, Promotes Nuclear Translocation of TFEB *via* Inhibition of the AMPK-MTORC1 Axis

Krishan, S.,[1] Sahni, S.[1,2,3*†] and Richardson, D.R.[1,4,5*†]
[†]Equal contribution as senior and corresponding author.
[1]*Molecular Pharmacology and Pathology Program, Department of Pathology and Bosch Institute, Medical Foundation Building (K25), University of Sydney, Sydney, New South Wales, 2006, Australia;*

[2]*Northern Clinical School, Faculty of Medicine and Health, University of Sydney, NSW, Australia.*

[3]*Kolling Institute of Medical Research, St Leonards, NSW, Australia.*

[4]*Department of Pathology and Biological Responses, Nagoya University Graduate School of Medicine, Nagoya 466-8550, Japan.*

[5]*Centre for Cancer Cell Biology and Drug Discovery, Griffith Institute for Drug Discovery, Griffith University, Nathan, Brisbane, Queensland, 4111, Australia.*

Running Title: TFEB and Dp44mT-Mediated Autophagy

***To whom correspondence should be addressed: Dr. Des R. Richardson,** Centre for Cancer Cell Biology and Drug Discovery, Griffith Institute for Drug Discovery, Griffith University, Nathan, Brisbane, Queensland, Australia. Email: d.richardson@griffith.edu.au; **Dr. Sumit Sahni**, Northern Clinical School, The University of Sydney, Sydney, New South Wales, Australia. Email: sumit.sahni@sydney.edu.au

Abstract

Di-2-pyridylketone 4,4-dimethyl-3-thiosemicarbazone (Dp44mT) and its analogues are potent anti-cancer agents through their ability to target lysosomes. Considering this, it was important to understand the mechanisms involved in the Dp44mT-mediated induction of autophagy and the role of 5'-adenosine monophosphate-activated protein kinase (AMPK) as a critical autophagic regulator. As such, this investigation examined AMPK's role in the regulation of the transcription factor EB (TFEB), which transcribes genes involved in autophagy and lysosome biosynthesis. For the first time, this study demonstrated that Dp44mT induces translocation of TFEB to the nucleus. Furthermore, Dp44mT-mediated nuclear translocation of TFEB was AMPK-dependent. Considering that: **(1)** the mammalian target of rapamycin complex 1 (mTORC1) plays an important

role in the regulation of TFEB; and **(2)** that AMPK is a known regulator of mTORC1, this study also elucidated the mechanisms through which Dp44mT regulates nuclear translocation of TFEB *via* AMPK. Silencing *AMPK* led to increased mTOR phosphorylation, that activates mTORC1. Since Dp44mT inhibits mTORC1 in an AMPK-dependent manner through raptor phosphorylation, Dp44mT is demonstrated to regulate TFEB translocation through dual mechanisms: AMPK activation, which inhibits mTOR, and inhibition of mTORC1 *via* phosphorylation of raptor. Collectively, Dp44mT-mediated activation of AMPK plays a crucial role in lysosomal biogenesis and TFEB function. As Dp44mT potently chelates copper and iron that are crucial for tumor growth, these studies provide insight into the regulatory mechanisms involved in intracellular clearance and energy metabolism that occur upon alterations in metal ion homeostasis.

1. Introduction

The catabolic enzyme, 5'-adenosine monophosphate-activated protein kinase (AMPK), plays a crucial role in the induction of autophagy [1, 2]. AMPK regulates autophagy *via* two mechanisms. First, AMPK phosphorylates Unc-51 like autophagy activating kinase 1 (ULK1), an important initiator of autophagy [3]. Second, AMPK is known to inhibit the mammalian target of rapamycin complex 1 (mTORC1) and mTORC1 inhibits the activation of ULK1, but also regulates the transcription of autophagy-related genes [3]. Previously our laboratory demonstrated that the anti-cancer agent, di-2-pyridylketone 4,4-dimethyl-3-thiosemicarbazone (Dp44mT; **Fig. 1A**), which demonstrates potent and selective anti-tumor activity, can activate ULK1 in an AMPK-dependent manner to induce autophagy [4].

Examining the mechanism of Dp44mT anti-cancer activity was important, as this agent belongs to the di-2-pyridylketone thiosemicarbazone (DpT) class of agents [5, 6], which have entered multi-center, Phase I clinical trials [7]. These compounds demonstrate marked potential through their ability to inhibit metastasis by up-regulating N-myc downstream regulated gene-1 [8, 9] and overcoming P-glycoprotein-mediated drug resistance [10, 11]. A key part of their efficacy is due to the so-called “double punch mechanism” [7]. This occurs when the agents first bind the essential cellular nutrients, iron and copper, which are critical for tumor growth (“first punch”), and then

form cytotoxic redox active iron, and particularly, copper complexes ("second punch"), that damage lysosomes [11, 12].

This latter mechanism induces lysosome membrane permeabilization and cathepsin release into the cytosol, which results in the cleavage of pro-apoptotic, Bid, that leads to apoptosis [11, 12]. The damage to the lysosome inhibits the fusion of the lysosome and the autophagosome, which prevents the completion of autophagy [13, 14]. Considering this, further studies are important to understand the mechanism of action of Dp44mT on the autophagic apparatus, as this understanding could lead to the development of agents with even greater efficacy and selectivity.

One of the regulators of autophagy-related gene transcription is the basic helix-loop-helix, leucine zipper transcription factor, namely transcription factor EB (TFEB) [15]. TFEB modulates the formation of autophagosomes and also the fusion of the autophagosome and lysosome [16]. Furthermore, TFEB also regulates lysosomal biogenesis through transcription of several lysosomal membrane proteins, including lysosomal hydrolase and components of the vacuolar H^+-ATPase complex [15, 17].

TFEB is regulated by nutrient fluctuations and cellular stress [18, 19] and is also modulated by the lysosome itself, as a response to lysosomal status through mTORC1 [20]. It is known that mTORC1 inhibits TFEB nuclear translocation, and additionally, mTORC1 has been identified on the lysosomal membrane [17]. Settembre *et al.* [20], showed that mTORC1 regulates the subcellular localization of TFEB including its translocation to the nucleus. In fact, mTORC1 targets Ser142 and Ser211 of TFEB for phosphorylation and this interaction occurs on the lysosomal membrane, as a response to lysosomal nutrient status [20]. TFEB has been reported to continuously cycle between the lysosome and the cytosol according to cellular nutrient levels with some fraction of TFEB being associated with lysosomes [20, 21].

Under normal nutritionally replete conditions, mTORC1 present on the lysosomal membrane phosphorylates TFEB and this phosphorylation inhibits the translocation of TFEB to the nucleus and prevents its function as a transcription factor [20]. Under cellular stress, such as low levels of ATP or glucose, mTORC1 is inhibited and TFEB then translocates to the nucleus to transcribe its target genes [20]. Once in the nucleus, TFEB is responsible for the transcription of autophagy-related genes and genes encoding lysosomal proteins [19]. These autophagy-related genes include *LC3B*, *P62*, *VPS11*, *VPS18*, *UVRAG*, *WIPI* and *ATG9B* [16]. Once transcribed and translated, the autophagy-related proteins are responsible for the formation of the double membrane autophagosome, in which damaged proteins and organelles are sequestered [22, 23]. The autophagosome loaded with cargo, fuses with the lysosome, resulting in the formation of the autolysosome [24]. The acidic hydrolases from lysosomes degrade the loaded cargo and release nutrients back into the cytoplasm for recycling, correcting the nutritional deficiency [24].

As lysosomes are important for the anti-tumor activity of Dp44mT [12] and because this agent is a potent chelator of the crucial cellular nutrients, iron and copper [6, 12, 25, 26], it is vital to investigate the role of TFEB in the regulation of the lysosome as a response to Dp44mT. TFEB plays a key role in the regulation of autophagy, but also organelle-specific autophagy, such as lipophagy and mitophagy [16, 27]. Since TFEB plays a role in the regulation of both autophagy and lysosomal biogenesis, modulating the transcriptional activity of TFEB enables regulation of lysosomal function and autophagy in response to environmental cues [19].

AMPK is known to inhibit mTORC1 activity both directly and indirectly, through raptor and tuberous sclerosis complex 2 (TSC2), respectively [28, 29]. AMPK increases the phosphorylation of raptor, which prevents the formation of the mTOR complex [28]. Additionally, AMPK also activates, TSC2, which is known to inhibit ras homolog enriched in brain (RHEB), an activator of mTOR [29, 30].

Our previous studies demonstrated that treatment of tumor cells with Dp44mT results in the phosphorylation of raptor in an AMPK-dependent manner [4]. From this observation it was hypothesized that Dp44mT-mediated activation of the AMPK pathway may lead to the inhibition of mTORC1. These events would subsequently activate TFEB, resulting in increased autophagy-related gene transcription and lysosomal biosynthesis. The current investigation aimed to examine this to understand the role of AMPK in the effect of Dp44mT on lysosomes and the pathways involved, as well as its effect on autophagy. Considering the potential of Dp44mT and its analogues as effective anti-cancer agents [5, 6], it was important to understand the mechanisms involved in Dp44mT-mediated autophagy [14, 31], and the role of AMPK as a key regulator of autophagy.

2. Materials and methods

2.1 Cell culture and treatment

PANC1 cells were grown and cultured as previously described [32]. The chelator, Dp44mT, was synthesized and characterized according to our established methodology [25, 33]. Cells were seeded into tissue culture plates and incubated until reaching approximately 80% confluence. These cells were then treated with either control medium or this medium containing Dp44mT at the indicated concentrations for 24 h/37^{o}C, or unless otherwise specified.

2.2 Gene silencing using siRNA

Cells were seeded onto plates and incubated for 24 h/37^{o}C, under the conditions described above in Section 2.1. These cells were then incubated with either 150 pmoles of negative control siRNA (NC siRNA; Cat. #AM4637; ThermoFisher Scientific, Waltham, MA, USA), *AMPKα1* siRNA, herein referred to *AMPK* siRNA (Cat. #143192; ThermoFisher Scientific), or *TFEB* siRNA (Cat. #s15495; ThermoFisher Scientific), and Lipofectamine 2000 in Opti-MEM (ThermoFisher Scientific) for 6 h/37^{o}C. The media was replaced, and cells were incubated for 48 h/37^{o}C, prior to treatment.

2.3 Protein extraction and western blotting

Protein was prepared using either whole cell lysates, as described previously [4, 34], or nuclear and cytoplasmic fractions were extracted using the NE-PER Nuclear and Cytoplasmic Extraction Reagent Kit (Pierce, IL, USA) following the manufacturer's protocol. The primary antibodies used included those against: p-AMPKα1 (Thr172; Cat. #2535; Cell Signaling Technology, Danvers, MA, USA); AMPKα (Cat. #2793; Cell Signaling Technology); LC3 (Cat. #PM036; MBL International, WOBURN, MA, USA); Beclin-1 (Cat. #3495, Cell Signaling Technology); TFEB (Cat. #37785; Cell Signaling Technology); LAMP2 (Cat. #ab25631; Abcam); cathepsin D (Cat. #ab72915; Abcam); p-mTOR (Ser2448; Cat. #2971; Cell Signaling Technology); mTOR (Cat. #2983; Cell Signaling Technology); p-TSC2 (Ser1387; Cat. #8350; Cell Signaling Technology); and TSC2 (Cat. #8350; Cell Signaling Technology). The primary antibodies were diluted 1:1000 in 5% (w/v) bovine serum albumin (BSA) in Tris-buffered saline (TBS; Sigma) containing 0.1% Tween-20 (TBST). As an assessment of equal protein-loading, membranes were probed for β-actin (Cat. #A1978; Sigma-Aldrich). The antibody against β-actin was diluted to 1:10,000 in 5% (w/v) non-fat milk in TBST. None of the agents tested had any effect on β-actin expression relative to the control, demonstrating its utility as an appropriate loading control.

Horseradish peroxidase (HRP)-conjugated anti-rabbit IgG and anti-mouse IgG from Sigma-Aldrich were used as secondary antibodies. These were diluted to 1:10,000 in 5% non-fat milk in TBST. The membranes were incubated with Luminata Crescendo Western HRP substrate (Cat. #WBLUR0100; Millipore, Billerica, MA, USA), or Luminata Forte Western HRP substrate (Cat. #WBLUF0100; Millipore). The chemiluminescence signals were captured using a ChemiDoc MP Imaging System (BioRad; NSW, Australia). Densitometric analysis was performed using ChemiDoc Image Lab Software (BioRad). Densitometry of bands was normalized to the corresponding β-actin standards.

2.4 Confocal immunofluorescence microscopy

Immunofluorescence using confocal microscopy was performed according to standard procedures [35, 36] . The slides were incubated with primary antibodies against rabbit anti-TFEB (Cat. #37785S; Cell Signaling Technology) in PBS (1% BSA) at 4 °C overnight. The slides were then washed in PBS and incubated with the secondary antibody anti-rabbit Ab conjugated to Alexa Fluor® 488 fluorescent dye (1:1000; Cat. #4412S; Cell Signaling) for 2 h/20 °C. Coverslips were mounted onto glass slides using ProLong® Gold Antifade Reagent with DAPI (Cat. #P36935; Life Technologies). Stained samples were examined with the Zeiss LSM 510 Meta Spectral Confocal Microscope using the 63 × oil objective. Images were captured with AxioVision Rel 4.8 software. The quantification of nuclear and cytoplasmic intensity was performed with the intensity ratio nuclei cytoplasmic tool using ImageJ (NIH, Maryland) and represents the average intensity/cell with 24-30 cells being quantified/condition over 3 experiments.

2.5 Statistics

Experimental data were compared using the Student's paired *t*-test. Results were considered statistically significant when $p < 0.05$. Results are presented as the mean ± standard error of the mean (SEM) of 3 experiments.

3. Results

3.1 Dp44mT induces translocation of TFEB from the cytoplasm to the nucleus

Research from our laboratory has convincingly demonstrated that Dp44mT activates autophagy in cancer cells [14, 31, 32]. As TFEB is a key regulator of transcription of autophagy-related genes [16], the goal of initial experiments was to examine the effect of Dp44mT on the sub-cellular localization of TFEB in the cytoplasm and nucleus. For these studies, the PANC1 cell-type was specifically chosen as our laboratory has previously characterized the response of these cells to Dp44mT, including its ability to activate AMPK, induce autophagy and elicit lysosomal membrane permeabilization [14, 31, 32]. Furthermore, our studies demonstrated that AMPK activation by Dp44mT in PANC1 cells was similar to other pancreatic cancer cell-types (*i.e.*, AsPC-1 and MIAPaCa-2) [32] and also to a panel of other tumor cell-types, including: MCF7 breast cancer

cells, HT29 colon carcinoma cells, DU145 prostate cancer cells and SK-N-MC neuroepithelioma cells [4]. These data indicate the response of PANC1 cells to Dp44mT is typical amongst a range of tumor cells, demonstrating their usefulness as a model for the current studies.

First, TFEB expression in PANC1 cells was assessed in the cytoplasm and nucleus, with fraction purity being determined by the expression of the cytoplasmic and nuclear proteins, glyceraldehyde-phosphate dehydrogenase (GAPDH) and histone deacetylase 1 (HDAC1; [37]), respectively. Two bands corresponding to TFEB were observed in the nuclear fraction at 65- and 70-kDa, with the latter band being the predominate isoform (**Fig. 1B**). The minor 65-kDa isoform was not always apparent in repeat experiments, probably due to it merging with the upper 70-kDa band.

The expression of TFEB was markedly and significantly ($p < 0.001$-0.01) higher levels in the nucleus relative to the cytoplasmic fraction (**Fig. 1B, C**), which is consistent with its known role as a transcription factor [15]. TFEB has been described as a low abundance protein in some cell-types [38]. The very low levels of TFEB in the cytoplasmic fraction was surprising and is further examined in the next stage of experimentation below in **Figure 2**. PANC1 cells incubated with serum-starved media were used as a positive control relative to incubation with medium containing serum, as serum-starvation is known to initiate nuclear translocation of TFEB [18, 38]. Under serum-starvation, there was a significant ($p < 0.01$) increase in the top band of TFEB at 70 kDa in the nuclear relative to cytoplasmic fraction (**Fig. 1B, C**). Hence, as this is an expected response that classically stimulates autophagy, the top band of TFEB at 70 kDa was used for quantification of the protein here and in all further studies, as this supported its role as the typical TFEB isoform involved in autophagy [18, 38].

PANC1 cells were then incubated with control medium or this medium containing increasing concentrations of Dp44mT (0-, 2.5-, or 5-μM) for 24 h/37 °C and the cytoplasmic and nuclear fractions then extracted and examined by western analysis (**Fig. 1D, E**). Again, TFEB levels in the nucleus in the control and Dp44mT-treated samples were markedly and significantly ($p < 0.001$)

greater in the nucleus relative to their respective cytoplasmic samples. There was a significant ($p < 0.05$) increase in TFEB levels (70-kDa) in the nucleus after incubation with Dp44mT (2.5- and 5-μM) *versus* the nuclear control (**Fig. 1D, E**). While the levels of TFEB at 70-kDa were increased by Dp44mT at both 2.5- and 5-μM relative to the respective control, a slight decrease in TFEB levels was observed at 5- relative to 2.5-μM. The reason for this response of TFEB to increasing Dp44mT concentration is currently unclear. However, it could be related to alterations in the metabolic response to this agent, which has been reported in this cell-type, where autophagy can convert to apoptosis under the stress induced by this anti-tumor agent [32]. The 65-kDa isoform of TFEB in the nucleus was shown to decrease as the concentration of Dp44mT increased (**Fig. 1D**), but because of the unknown significance of this isoform, it is not considered further and was not quantitated.

Collectively, these results in **Figure 1B-E** indicate that Dp44mT increased nuclear translocation of the 70-kDa TFEB isoform that responded to nutrient deprivation (*i.e.*, serum starvation in **Fig. 1B, C** and iron and copper chelation by Dp44mT in **Fig. 1D, E**).

3.2 Confocal microscopy identifies cytosolic TFEB in punctate foci in cells that translocate to nuclei upon Dp44mT treatment

Considering these results from western analysis in **Figs. 1D, E**, the intracellular localization of TFEB was also examined using a different antibody that is recommended for immunofluorescence using confocal microscopy (**Fig. 2**). In these studies, PANC1 cells were incubated for 24 h/37°C with 0 (Control), 1.25-, 2.5- or 5-μM Dp44mT. The intracellular localization of TFEB was demonstrated to be significantly ($p < 0.001$) higher in the cytoplasm relative to the nucleus under control conditions (**Fig. 2A, B**). Clearly, the antibody used for immunofluorescence appeared to demonstrate far greater sensitivity in detecting “cytosolic” TFEB relative to the antibody implemented for western analysis (**Fig. 1B, D**). However, from confocal microscopy analysis,

TFEB appeared in the cytoplasm as granular puncta, suggesting that it may be associated with organelles, rather than being "free" in the cytosol (see magnified image; **Fig. 2A**).

In fact, TFEB has been reported to continuously cycle between lysosomes, the cytosol and the nucleus according to cellular nutrient levels [20, 21]. As such, the granular puncta of TFEB in cells could indicate its association with lysosomes or associated organelle systems (*e.g.,* endoplasmic reticulum, vesicles, *etc.*) that enable the known inter-organelle shuttling of TFEB. Increased amino acid levels lead to the interaction of TFEB with active Rag guanosine triphosphatases (GTPases) to promote recruitment of TFEB to lysosomes [21]. This results in mTORC1-dependent phosphorylation and inhibition of TFEB on lysosomes [21] and may explain the lower levels of TFEB in the nucleus under control conditions and the granular appearance of cytosolic TFEB (**Fig. 2A**). Hence, the cytoplasmic fraction of TFEB in **Figure 1B, D** probably does not correlate to the cytosolic TFEB observed *via* confocal microscopy, which includes organelle interactions (**Fig. 2A**).

Nonetheless, after incubation of cells with Dp44mT at all concentrations (1.25-5 μM), there was a significant ($p < 0.001$-0.05) increase in perinuclear and nuclear-associated TFEB and a marked decrease in cytosolic TFEB expression (**Fig. 2A, B**). These results are consistent with the western analysis in **Figure 1D, E**. In fact, after Dp44mT treatment, TFEB was localized in the nucleus as granular occlusions and also in a perinuclear location (**Fig. 2A**). Some evidence of plasma membrane-associated TFEB also was observed after Dp44mT treatment, with a definite, pronounced decrease in total cellular TFEB being identified after incubation with all Dp44mT concentrations relative to the control (**Fig. 2A**).

Collectively, these data in **Figures 1** and **2** indicate that incubation of PANC1 cells with Dp44mT leads to perinuclear and nuclear translocation of the master transcriptional regulator of autophagy, TFEB.

3.3 AMPK expression is essential for the nuclear translocation of TFEB

It is well known that AMPK plays a role in the initiation of autophagy in cancer cells through activation of ULK1 and inhibition of mTORC1 [3]. Furthermore, since the nuclear translocation of TFEB is inhibited by mTORC1 [20], this study aimed to examine the role of Dp44mT-mediated activation of the AMPK pathway in the nuclear localization of TFEB (**Fig. 3**).

To investigate this, PANC-1 cells were incubated for 48 h/37 °C with either negative control (NC) siRNA or *AMPK* siRNA, followed by incubation with control medium or this medium containing Dp44mT (2.5 μM) for 24 h/37 °C (**Fig. 3A, B**). This concentration of Dp44mT was implemented as it demonstrated maximal ability to induce nuclear translocation of TFEB (**Fig. 2B**) without evidence of cytotoxicity after a 24 h incubation and has also been previously demonstrated to activate AMPK [4]. Sub-cellular localization of TFEB was again examined using confocal immunofluorescence microscopy, with the granular, punctate nature of TFEB again being evident in the magnified image (**Fig. 3A**). In control cells treated with the NC siRNA, TFEB was again observed to be at significantly ($p < 0.05$) greater levels in the cytoplasm relative to the nucleus (**Fig. 3A, B**), as found in **Figure 2A, B**. In contrast, incubation of NC siRNA-treated cells with Dp44mT (2.5 μM), resulted in a significant ($p < 0.05$) increase in perinuclear and nuclear TFEB compared to the control, and a significant ($p < 0.05$) decrease of TFEB in the cytoplasm relative to the control (**Fig. 3A, B**). As observed in **Figure 2A, B** there was also a decrease in total TFEB fluorescence after Dp44mT treatment relative to the control in NC siRNA-treated cells (**Fig. 3A**).

After silencing *AMPK* in PANC1 cells and then treating them with either the control medium or this medium containing Dp44mT, there was a marked decrease in total cellular TFEB relative to control cells incubated with NC siRNA (**Fig. 3A**). Relative to the control in NC siRNA-treated cells, silencing *AMPK* in control cells led to a decrease in cytosolic TFEB and a slight increase in nuclear TFEB (**Fig. 3A, B**). Incubation of *AMPK* siRNA-treated cells with Dp44mT (2.5 μM) had no significant ($p > 0.05$) effect on the subcellular localization of TFEB in the nucleus or cytoplasm

compared to the respective control (**Fig. 3A, B**). Importantly, relative to NC siRNA-treated cells incubated with Dp44mT, *AMPK* silencing largely prevented the ability of Dp44mT to increase nuclear levels of TFEB.

These results in **Figure 3** indicate that AMPK expression plays a role in the ability of Dp44mT to induce nuclear translocation of TFEB, suggesting the known activation of AMPK by Dp44mT [4] could be involved in its ability to result in nuclear translocation of TFEB.

3.4 Dp44mT increases p-TSC levels and AMPK inhibits mTOR phosphorylation-independent of TSC2

As demonstrated in the previous section, AMPK played an important role in the regulation of the sub-cellular localization of TFEB in response to Dp44mT (**Fig. 3**). This effect can be hypothesized to be due to AMPK's ability to inhibit mTOR phosphorylation *via* TSC2 [29]. AMPK is known to supresses mTORC1 activity through dual mechanisms. First, AMPK inhibits the formation of the mTORC1 complex through phosphorylation of raptor [28]. Second, AMPK also phosphorylates TSC2, which subsequently decreases mTOR phosphorylation and its activation [29, 30]. Our laboratory demonstrated that Dp44mT markedly increases AMPK activation and raptor phosphorylation, which are known to prevent the formation of the mTORC1 complex that inhibits protein synthesis [4]. However, the effect of Dp44mT on mTOR and TSC2 phosphorylation was not examined, and is now investigated here, together with the role of AMPK in this regulation (**Fig. 4**).

In these studies, PANC1 cells were incubated for 48 h/37°C with either NC siRNA or *AMPK* siRNA, followed by a 24 h/37°C incubation with control medium or this medium containing Dp44mT (2.5 μM). As shown by our laboratory previously [4], Dp44mT significantly ($p < 0.05$) inhibited total AMPK protein level and also significantly ($p < 0.05$) increased p-AMPK (Thr172) relative to the respective controls after incubation with NC siRNA (**Fig. 4A, B*i,ii***). As a control for

AMPK silencing, total AMPK and p-AMPK was investigated, with *AMPK* siRNA significantly ($p <$ 0.01-0.001) decreasing total and p-AMPK levels in the presence or absence of Dp44mT relative to NC siRNA (**Fig. 4A, B*i,ii***).

Examining p-TSC2 (Ser1387) levels, there was a significant ($p < 0.05$) increase after incubation with Dp44mT compared to the control in NC siRNA-treated cells (**Fig. 4A, B*iii***). In contrast, p-TSC2 levels were significantly ($p < 0.05$) decreased in *AMPK*-silenced cells after incubation with the control or Dp44mT relative to the respective treatments in NC siRNA cells (**Fig. 4A, B*iii***). However, despite *AMPK*-silencing, there was a significant ($p < 0.05$) increase in p-TSC2 levels after incubation with Dp44mT relative to the respective control (**Fig. 4A, B*iii***). Assessing total TSC2 levels, there was a significant ($p <$ 0.01-0.05) decrease in TSC2 levels after incubation with Dp44mT in both NC- and -*AMPK* siRNA treated cells, compared to their respective controls (**Fig. 4A, B*iv***). The effect of Dp44mT on decreasing TSC2 was significantly ($p < 0.05$) greater after *AMPK* siRNA relative to the NC siRNA treatment.

There was a marked and significant ($p < 0.05$) increase in the p-TSC2/TSC2 ratio after incubation with Dp44mT, which occurred to a similar extent in both NC siRNA cells and *AMPK* siRNA cells, compared to the respective control (**Fig. 4A, B*v***). Interestingly, despite the increase in p-TSC2 levels after incubation with Dp44mT in the NC siRNA cells (**Fig. 4A, B*iii***), there was only a slight ($p > 0.05$) increase of p-mTOR (Ser2448) levels after incubation with Dp44mT compared to control cells (**Fig. 4A, B*vi***). However, there was a pronounced and significant ($p <$ 0.01-0.05) increase in p-mTOR levels in *AMPK*-silenced cells for both the control- and Dp44mT-treatment, compared to the respective NC siRNA-treated cells (**Fig. 4A, B*vi***). This observation suggests that AMPK expression inhibits mTOR phosphorylation irrespective of Dp44mT. In contrast, *AMPK*-silencing resulted in a significant ($p <$ 0.01-0.05) decrease in mTOR levels for both the control and Dp44mT compared to the analogous treatment of NC siRNA cells (**Fig. 4A, Bv*ii***). Due to these latter alterations, there was

a significant (p < 0.01-0.05) increase in p-mTOR/mTOR ratio in *AMPK*-silenced cells for both the control and Dp44mT-treatment compared to NC siRNA cells (**Fig. 4A, B*viii***).

Collectively, these results indicate that: **(1)** Dp44mT increases p-TSC2 levels irrespective of AMPK expression, and increased p-TSC2 is known to inhibit mTORC1 formation; and **(2)** *AMPK* silencing increases p-mTOR in the presence or absence of Dp44mT, implying that AMPK inhibits p-mTOR in the presence or absence of Dp44mT. Hence, Dp44mT will lead to autophagy through both these mechanisms.

3.5 TFEB plays a role in Dp44mT-mediated autophagy

Our previous studies have clearly demonstrated that through its ability to bind the crucial cellular nutrients, iron and copper, Dp44mT activates AMPK to induce autophagy [4]. In the current investigation, *AMPK* silencing was demonstrated to largely prevent the ability of Dp44mT to increase nuclear TFEB levels (**Fig. 3**), implying a role for AMPK in this process. Since AMPK is known to play a role in the regulation of TFEB [20], the role of TFEB in Dp44mT-mediated autophagy was also examined. These studies were performed in the presence or absence of the late-stage autophagic inhibitor, Bafilomycin A1 (Baf A1; **Fig. 5**) [39]. Autophagosome levels were assessed by examining the expression of its classical marker, microtubule-associated protein 1 light chain 3 (LC3-II), which is present on the autophagosome membrane throughout its life [40]. Initially, PANC1 cells were incubated with either NC siRNA or *TFEB* siRNA for 48 h/37°C, followed by incubation with Dp44mT (2.5 μM), Baf A1 (100 nM), or both, for 24 h/37°C. These conditions with Baf A1 have previously been demonstrated by our laboratory to optimally inhibit autophagosome formation in PANC1 cells [31].

In these experiments, Dp44mT markedly and significantly (p < 0.001) decreased total cellular TFEB expression in NC siRNA-treated cells in the absence of Baf A1 *versus* the respective controls (**Fig. 5A, B*i***). A similar decrease in total cellular TFEB after incubation with Dp44mT was

demonstrated in **Figures 2** and **3**. Silencing *TFEB* caused a pronounced and significant ($p < 0.001$) decrease in its levels in the presence and absence of Dp44mT relative to the respective NC siRNA conditions (**Fig. 5A, B*i***). Examining LC3-I levels in the absence of Baf A1, both NC siRNA and TFEB siRNA did not result in any significant ($p > 0.05$) alteration relative to the respective controls (**Fig. 5A, B*ii***). After incubation of Baf A1 with the NC siRNA- or *TFEB* siRNA-treated cells, there was no significant ($p > 0.05$) change in LC3-I level in either the control- or Dp44mT-treated groups relative to the control of the NC siRNA group not treated with Baf A1 (**Fig. 5A, B*ii***).

Assessing LC3-II levels in cells not treated with Baf A1, there was a significant ($p < 0.01$-0.05) increase in the NC siRNA- and TFEB siRNA-treated cells after incubation with Dp44mT relative to the control (**Fig. 5A, B*iii***). This increase in LC3-II after incubation with Dp44mT could be due to either increased autophagosome formation or a decrease in lysosome-mediated autophagosome degradation. To further elucidate this mechanism cells were also co-incubated with the late-stage autophagy inhibitor Baf A1.

Incubation of NC siRNA-treated cells with Baf A1 in the absence of Dp44mT resulted in a significant ($p < 0.01$) increase in the level of LC3-II compared to the relative NC siRNA-treated control cells (**Fig. 5A, B*iii***). Interestingly, while there was a significant ($p < 0.05$) increase in LC3-II levels in the *TFEB*-silenced and Baf A1-treated cells after incubation with Dp44mT relative to the control (**Fig. 5A, B*iii***), this increase was significantly ($p < 0.05$) less pronounced than that observed with Dp44mT in NC siRNA-treated cells (**Fig. 5A, B*iii***). This observation suggests that silencing *TFEB* suppressed the Dp44mT-mediated initiation of autophagy.

In summary, these results in **Figure 5A, B** indicate that Dp44mT induces autophagy in a TFEB-dependent manner.

3.6 Dp44mT suppresses Beclin-1 expression in the absence and presence of TFEB

We further examined the role of TFEB in the regulation of Beclin-1 (**Fig. 5C, D**), another regulator of the autophagy process [41]. PANC1 cells were incubated for 48 h/37°C with either NC siRNA or *TFEB* siRNA, followed by incubation for 24 h/37°C in the absence and presence Dp44mT (2.5 μM). The levels of TFEB and Beclin-1 were then analyzed by western blotting. Incubation with Dp44mT significantly ($p < 0.001$) decreased total TFEB expression after incubation with NC siRNA or *TFEB* siRNA relative to the NC siRNA-treated control (**Fig. 5C, D*i***). Silencing *TFEB* resulted in a marked and significant ($p < 0.001$) decrease in its expression relative to the respective NC siRNA (**Fig. 5C, D*i***). There was a significant ($p < 0.01$-0.05) decrease in Beclin-1 levels in NC siRNA-treated cells and TFEB siRNA-treated cells after incubation with Dp44mT relative to the respective controls (**Fig. 5C, D*ii***). Silencing *TFEB* expression resulted in a significant ($p < 0.05$) increase in Beclin-1 levels for both the control and Dp44mT-treatments relative to the respective treatments after incubation with the NC siRNA (**Fig. 5C, D*ii***).

In summary, the results in **Figure 5C, D** demonstrate that the suppression of Beclin-1 expression by Dp44mT is TFEB-independent.

3.7 AMPK and Dp44mT regulate levels of the lysosomal markers, LAMP2 and cathepsin D

Apart from regulating autophagy, TFEB plays a key role in lysosomal biosynthesis due to the transcription of several lysosomal genes [15, 17]. One of the major mechanisms of action for Dp44mT is through its ability to induce lysosomal membrane permeabilization [7, 12, 14]. We previously demonstrated that *AMPK*-silencing results in decreased lysosomal membrane permeabilization and stabilization of lysosomes in PANC1 cells [32]. The current study examined the effect of *AMPK*-silencing on the well-known lysosomal markers, lysosome-associated membrane protein 2 (LAMP2; [42]), and the soluble lysosomal protease, cathepsin D ([43]; **Fig. 6**).

In these studies, PANC1 cells were incubated for 48 h/37°C with either NC siRNA or *AMPK* siRNA, prior to incubation in the absence or presence of Dp44mT (2.5 μM; 24 h). Again, total

AMPK was used as a control with *AMPK* siRNA significantly ($p < 0.001$-0.01) decreasing its levels (**Fig. 6A, B*i***). Furthermore, as shown previously [4], total AMPK and its levels were significantly ($p < 0.001$-0.01) decreased by Dp44mT after treatment of PANC1 cells with NC siRNA and especially *AMPK* siRNA (**Fig. 6A, B*i***).

There was a slight, but significant ($p < 0.05$) decrease in LAMP2 levels in NC siRNA-treated cells after incubation with Dp44mT compared to the control (**Fig. 6A, B*ii***). In contrast, LAMP2 levels were significantly ($p < 0.01$) increased in *AMPK*-silenced control cells compared to NC siRNA-treated control cells (**Fig. 6A, C*ii***). This observation may be related to our previously reported finding that *AMPK* silencing stabilizes the lysosome in PANC-1 cells due to increased cholesterol levels [32]. There was a significant ($p < 0.05$) decrease in LAMP2 expression after incubation of PANC1 cells with Dp44mT after *AMPK*-silencing, compared to the respective control (**Fig. 6A, B*ii***), which may be again related to the ability of Dp44mT to induce lysosomal membrane permeabilization [12, 14].

Examining cathepsin D levels in NC siRNA-treated cells, there was a significant ($p < 0.05$) decrease after incubation with Dp44mT *versus* the control (**Fig. 6A, B*iii***). Silencing *AMPK* resulted in a slight, but significant ($p < 0.01$) increase of cathepsin D levels in the control treatment relative to the NC siRNA-treated control. A more pronounced and significant ($p < 0.05$) increase in cathepsin D expression was observed with *AMPK* silencing after Dp44mT treatment relative to the analogously treated NC siRNA cells (**Fig. 6A, B*iii***).

In summary, silencing *AMPK* led to increased lysosomal LAMP2 and cathepsin D in control cells, while *AMPK* silenced cells incubated with Dp44mT resulted in either decreased LAMP2 or increased cathepsin D expression *versus* the relative control. The difference in response may be related to LAMP2 being a membrane-bound lysosomal protein, while cathepsin D is a soluble lysosomal enzyme [42, 43].

3.8 TFEB and Dp44mT regulate levels of the lysosomal markers, LAMP2 and cathepsin D

The role of TFEB expression in the regulation of LAMP2 and cathepsin D levels by Dp44mT was also examined using western blotting (**Fig. 6C, D*i-iii***). PANC1 cells were treated with NC siRNA or *TFEB* siRNA for 48 h, followed by an incubation in the absence or presence of Dp44mT (2.5 μM) for 24 h. As shown in **Figures 2A, B, 3A, B, and 5A, B*i***, again total TFEB was significantly ($p < 0.001$-0.05) decreased by Dp44mT in cells incubated with NC siRNA and especially *AMPK* siRNA (**Fig. 6C, D*i***). Incubation of PANC1 cells with *TFEB* siRNA followed by with the control or Dp44mT resulted in a marked and significant ($p < 0.001$) decrease in its levels (**Fig. 6C, D*i***).

Assessing NC siRNA-treated cells, there was a significant ($p < 0.001$-0.05) decrease in both LAMP2 and cathepsin D expression after incubation with Dp44mT relative to the control (**Fig. 6C, D*ii, iii***), as shown above (**Fig. 6A, B*ii, iii***). This effect is again possibly due to the known ability of Dp44mT to induce lysosomal membrane permeabilization [7, 12, 14]. In *TFEB*-silenced cells, there was a significant ($p < 0.001$) decrease in the levels of both LAMP2 and cathepsin D after incubation with the control or Dp44mT relative to the respective treatments incubated with NC siRNA (**Fig. 6C, D*ii, iii***). However, incubation with Dp44mT did not lead to any significant ($p > 0.05$) alteration in LAMP2 or cathepsin D levels compared to the respective control after *TFEB*-silencing (**Fig. 6C, D*ii***). Collectively, these results suggest that TFEB expression plays a role in the regulation of LAMP2 and cathepsin D, both being targets of this transcription factor [44]. Moreover, the decrease in LAMP2 and cathepsin D by Dp44mT could be related to the decreased total levels of TFEB induced by this agent (**Figs. 2A,B, 3A,B, 5A,B*i*, 6C,D*i***), or its ability to increase lysosomal membrane permeabilization [7, 12, 14].

4 Discussion

TFEB plays a role as a master regulator of autophagy and also lysosomal biosynthesis as it is responsible for the transcription of multiple lysosomal genes [19, 20]. One of the major mechanisms of anti-proliferative activity of Dp44mT involves lysosomal membrane permeabilization [7, 12, 14].

Such lysosomal damage impairs autophagy, as the lysosome and the autophagosome are no longer able to fuse to form the autolysosome resulting in dysfunctional autophagy [14].

TFEB acts in the nucleus and its localization is regulated by mTORC1 activity [20]. For the first time, we demonstrate that Dp44mT induces increased nuclear TFEB, although total cellular levels of TFEB were also suppressed. The increased nuclear TFEB may play a role in the increased autophagy observed after incubation with Dp44mT [14, 31]. Considering this, it is well known that TFEB regulates the transcription of autophagy-related genes [19]. In our studies, we demonstrated that LC3-II levels were decreased in *TFEB*-silenced cells and Dp44mT was able increase LC3-II levels. However, silencing *TFEB* suppressed the ability of Dp44mT to increase LC3-II levels in the presence of the late-stage autophagy inhibitor, Baf A1, suggesting a decrease in autophagy flux, and thus, these studies demonstrate a role for TFEB in promoting Dp44mT-mediated autophagic initiation.

Previous investigations from our laboratory demonstrated that Dp44mT can increase the phosphorylation of raptor [4], which is known to inhibit the formation of mTORC1 that plays a crucial role in protein synthesis and proliferation and negatively regulates catabolic processes such as autophagy [45]. This inhibition of mTORC1 activity by Dp44mT, could potentially lead to TFEB activation, as mTORC1 is known to suppress nuclear translocation of TFEB [20].

Our previous studies demonstrated that the Dp44mT-mediated phosphorylation of raptor was AMPK-dependent [4]. Herein, we have demonstrated that *AMPK* silencing increases phosphorylation of mTOR. This result implies that AMPK activation and expression inhibits mTOR activation, which would prevent mTORC1 formation and result in nuclear translocation of TFEB. We previously demonstrated that Dp44mT markedly promotes AMPK activation [4], and in the current study, this agent increased p-TSC2 levels. Hence, Dp44mT regulates subcellular localization of TFEB by inhibiting both arms of mTORC1 activation, namely by: **(1)** inhibiting

mTORC1 formation *via* the phosphorylation of raptor [4]; and **(2)** by activation of the AMPK pathway, which leads to phosphorylation of TSC2 at Ser1387, preventing mTORC1 formation that is vital for protein synthesis and growth. Our previous studies have demonstrated that cytotoxic iron chelators markedly inhibit protein synthesis in a wide variety of tumor cells *in vitro* [46], although the exact molecular mechanism had not been elucidated until this investigation.

The identification of TFEB as a global modulator of intracellular clearance and energy metabolism, through the regulation of genes involved in the lysosomal–autophagic pathways, has provided insights into the mechanism by which the cell responds to environmental cues such as nutrient availability. However, the effect of chelation of the essential nutrients iron and copper has not been examined in terms of these regulatory pathways. As Dp44mT is a potent chelator of both these metal ions [6, 12], the current studies provide insight also into the regulatory responses that occur upon alterations in metal ion homeostasis.

Constitutively enhanced TFEB activity has been linked to increased tumorigenesis, as in the case of renal clear cell carcinoma [47, 48]. Furthermore, induction of autophagy by activation of microphthalmia-associated transcription factor (MiT) genes, including TFEB, has been found to have an important role in pancreatic cancer [49], which is relevant to the current investigation assessing PANC1 pancreatic cancer cells. As such, the ability of Dp44mT to: **(1)** inhibit mTORC1, which is key to protein synthesis and proliferation [45]; and **(2)** to stimulate the initiation of autophagy, that is then targeted *via* lysosomal membrane permeabilization [12]; explains, in part, the potent anti-tumor activity of this class of thiosemicarbazones [5-7].

Despite the increase in nuclear TFEB after incubation with Dp44mT (**Figs. 1C,D, 2A,B, 3A,B**), it was of interest to note that several well-characterized downstream targets of TFEB, namely the lysosomal proteins, LAMP2 and cathepsin D, were down-regulated by Dp44mT. The decrease in the expression of these proteins could be due to the decreased protein synthesis induced by the

ability of Dp44mT to inhibit mTORC1 formation. Alternatively, or together with this latter effect, the decrease in lysosomal LAMP2 and cathepsin D could be due to the ability of Dp44mT to induce lysosomal membrane permeabilization. In fact, previous studies using immunofluorescence have demonstrated a decrease in lysosomal LAMP2 and cathepsin D after incubation with cells with Dp44mT and its closely related analogues [50].

5. Summary and Conclusions

The present work demonstrates that Dp44mT-mediated activation of the AMPK pathway plays a role in lysosomal biogenesis and function of TFEB (**Fig. 7**). This agent was demonstrated to increase nuclear TFEB, which plays a key role in the transcription of genes involved in both lysosomal biogenesis and autophagy. Dp44mT regulates TFEB by inhibiting both arms of mTORC1 activation. This occurs through Dp44mT activating AMPK, which results in: **(1)** phosphorylation of raptor [4]; and **(2)** TSC2 phosphorylation, which prevents mTORC1 formation that is critical for protein synthesis and proliferation.

Collectively, together with our previous studies [12], the current investigation demonstrates that Dp44mT increases TFEB nuclear localization to induce autophagy, which is then targeted by this agent to provoke lysosomal membrane permeabilization [7, 12, 14]. This mechanism explains, in part, the marked and promising anti-tumor efficacy of this class of thiosemicarbazones. This insight into the role of TFEB in Dp44mT-mediated autophagy could result in better anti-cancer treatment strategies in the future.

Acknowledgments

This work was supported by a National Health and Medical Research Council of Australia (NHMRC) Project Grant (1002867) and NHMRC Senior Principal Research Fellowships (APP1062607 and APP1159596) to D.R.R. S.S. would like to thank Mr. Guy Boncardo for the Boncardo Pancreatic Cancer Fellowship. S.S. would also like to thank AMP Foundation for the AMP Tomorrow Grant and Cancer Australia and Cure Cancer Australia for a Young Investigator PdCCRs grant. S.S. acknowledges support from Love Your Sister Foundation and the National

Breast Cancer Foundation Australia for an IIRS grant [IIRS-19-058].

Disclosures

None

References

[1] K.S. Choi, Autophagy and cancer, Exp. Mol. Med. 44 (2012) 109-20.

[2] S. Krishan, D.R. Richardson, S. Sahni, Adenosine monophosphate-activated kinase and its key role in catabolism: structure, regulation, biological activity, and pharmacological activation, Mol. Pharmacol. 87 (2015) 363-77.

[3] J. Kim, M. Kundu, B. Viollet, K.L. Guan, AMPK and mTOR regulate autophagy through direct phosphorylation of Ulk1, Nat. Cell Biol. 13 (2011) 132-41.

[4] S. Krishan, D.R. Richardson, S. Sahni, The anticancer agent, di-2-pyridylketone 4,4-dimethyl-3-thiosemicarbazone (Dp44mT), up-regulates the AMPK-dependent energy homeostasis pathway in cancer cells, Biochim. Biophys. Acta 1863 (2016) 2916-2933.

[5] M. Whitnall, J. Howard, P. Ponka, D.R. Richardson, A class of iron chelators with a wide spectrum of potent antitumor activity that overcomes resistance to chemotherapeutics, Proceedings of the National Academy of Sciences 103 (2006) 14901-14906.

[6] J. Yuan, D.B. Lovejoy, D.R. Richardson, Novel di-2-pyridyl-derived iron chelators with marked and selective antitumor activity: in vitro and in vivo assessment, Blood 104 (2004) 1450-1458.

[7] P.J. Jansson, D.S. Kalinowski, D.J. Lane, Z. Kovacevic, N.A. Seebacher, L. Fouani, S. Sahni, A.M. Merlot, D.R. Richardson, The renaissance of polypharmacology in the development of anti-cancer therapeutics: Inhibition of the "triad of death" in cancer by di-2-pyridylketone thiosemicarbazones, Pharmacol. Res. 100 (2015) 255-60.

[8] N.T. Le, D.R. Richardson, Iron chelators with high antiproliferative activity up-regulate the expression of a growth inhibitory and metastasis suppressor gene: a link between iron metabolism and proliferation, Blood 104 (2004) 2967-75.

[9] W. Liu, F. Xing, M. Iiizumi-Gairani, H. Okuda, M. Watabe, S.K. Pai, P.R. Pandey, S. Hirota, A. Kobayashi, Y.Y. Mo, K. Fukuda, Y. Li, K. Watabe, N-myc downstream regulated gene 1 modulates

Wnt-β-catenin signalling and pleiotropically suppresses metastasis, EMBO Mol. Med. 4 (2012) 93-108.

[10] P.J. Jansson, T. Yamagishi, A. Arvind, N. Seebacher, E. Gutierrez, A. Stacy, S. Maleki, D. Sharp, S. Sahni, D.R. Richardson, Di-2-pyridylketone 4, 4-dimethyl-3-thiosemicarbazone (Dp44mT) overcomes multidrug resistance by a novel mechanism involving the hijacking of lysosomal P-glycoprotein (Pgp), J. Biol. Chem. 290 (2015) 9588-9603.

[11] N.A. Seebacher, D.R. Richardson, P.J. Jansson, A mechanism for overcoming P-glycoprotein-mediated drug resistance: novel combination therapy that releases stored doxorubicin from lysosomes via lysosomal permeabilization using Dp44mT or DpC, Cell Death Dis. 7 (2016) e2510.

[12] D.B. Lovejoy, P.J. Jansson, U.T. Brunk, J. Wong, P. Ponka, D.R. Richardson, Antitumor activity of metal-chelating compound Dp44mT is mediated by formation of a redox-active copper complex that accumulates in lysosomes, Cancer Res. 71 (2011) 5871-80.

[13] S. Sahni, J. Gillson, K.C. Park, S. Chiang, L.Y.W. Leck, P.J. Jansson, D.R. Richardson, NDRG1 suppresses basal and hypoxia-induced autophagy at both the initiation and degradation stages and sensitizes pancreatic cancer cells to lysosomal membrane permeabilization, Biochim Biophys Acta Gen Subj 1864 (2020) 129625.

[14] E. Gutierrez, D.R. Richardson, P.J. Jansson, The anticancer agent di-2-pyridylketone 4,4-dimethyl-3-thiosemicarbazone (Dp44mT) overcomes prosurvival autophagy by two mechanisms: persistent induction of autophagosome synthesis and impairment of lysosomal integrity, J. Biol. Chem. 289 (2014) 33568-89.

[15] M. Sardiello, M. Palmieri, A. di Ronza, D.L. Medina, M. Valenza, V.A. Gennarino, C. Di Malta, F. Donaudy, V. Embrione, R.S. Polishchuk, A gene network regulating lysosomal biogenesis and function, Science 325 (2009) 473-477.

[16] C. Settembre, C. Di Malta, V.A. Polito, M.G. Arencibia, F. Vetrini, S. Erdin, S.U. Erdin, T. Huynh, D. Medina, P. Colella, TFEB links autophagy to lysosomal biogenesis, Science 332 (2011) 1429-1433.

[17] R. Zoncu, L. Bar-Peled, A. Efeyan, S. Wang, Y. Sancak, D.M. Sabatini, mTORC1 senses lysosomal amino acids through an inside-out mechanism that requires the vacuolar H+-ATPase, Science 334 (2011) 678-683.

[18] L. Li, H.J. Friedrichsen, S. Andrews, S. Picaud, L. Volpon, K. Ngeow, G. Berridge, R. Fischer, K.L.B. Borden, P. Filippakopoulos, C.R. Goding, A TFEB nuclear export signal integrates amino acid supply and glucose availability, Nat. Commun. 9 (2018) 2685.

[19] G. Napolitano, A. Ballabio, TFEB at a glance, J. Cell Sci. 129 (2016) 2475-81.

[20] C. Settembre, R. Zoncu, D.L. Medina, F. Vetrini, S. Erdin, S. Erdin, T. Huynh, M. Ferron, G. Karsenty, M.C. Vellard, A lysosome- to- nucleus signalling mechanism senses and regulates the lysosome via mTOR and TFEB, EMBO J. 31 (2012) 1095-1108.

[21] J.A. Martina, Y. Chen, M. Gucek, R. Puertollano, MTORC1 functions as a transcriptional regulator of autophagy by preventing nuclear transport of TFEB, Autophagy 8 (2012) 903-14.

[22] Y. Ohsumi, Historical landmarks of autophagy research, Cell Res. 24 (2014) 9-23.

[23] Z. Xie, U. Nair, D.J. Klionsky, Atg8 controls phagophore expansion during autophagosome formation, Mol. Biol. Cell 19 (2008) 3290-8.

[24] A.U. Arstila, B.F. Trump, Studies on cellular autophagocytosis. The formation of autophagic vacuoles in the liver after glucagon administration, Am. J. Pathol. 53 (1968) 687-733.

[25] D.R. Richardson, P.C. Sharpe, D.B. Lovejoy, D. Senaratne, D.S. Kalinowski, M. Islam, P.V. Bernhardt, Dipyridyl thiosemicarbazone chelators with potent and selective antitumor activity form iron complexes with redox activity, J. Med. Chem. 49 (2006) 6510-21.

[26] P.J. Jansson, P.C. Sharpe, P.V. Bernhardt, D.R. Richardson, Novel thiosemicarbazones of the ApT and DpT series and their copper complexes: identification of pronounced redox activity and characterization of their antitumor activity, J. Med. Chem. 53 (2010) 5759-69.

[27] C.L. Nezich, C. Wang, A.I. Fogel, R.J. Youle, MiT/TFE transcription factors are activated during mitophagy downstream of Parkin and Atg5, J. Cell Biol. 210 (2015) 435-450.

[28] D.M. Gwinn, D.B. Shackelford, D.F. Egan, M.M. Mihaylova, A. Mery, D.S. Vasquez, B.E. Turk, R.J. Shaw, AMPK phosphorylation of raptor mediates a metabolic checkpoint, Mol. Cell 30 (2008) 214-26.

[29] R.J. Shaw, LKB1 and AMP-activated protein kinase control of mTOR signalling and growth, Acta Physiol. 196 (2009) 65-80.

[30] K. Inoki, Y. Li, T. Xu, K.L. Guan, Rheb GTPase is a direct target of TSC2 GAP activity and regulates mTOR signaling, Genes Dev. 17 (2003) 1829-34.

[31] S. Sahni, D.H. Bae, D.J. Lane, Z. Kovacevic, D.S. Kalinowski, P.J. Jansson, D.R. Richardson, The metastasis suppressor, N-myc downstream-regulated gene 1 (NDRG1), inhibits stress-induced autophagy in cancer cells, J. Biol. Chem. 289 (2014) 9692-9709.

[32] S. Krishan, S. Sahni, L.Y.W. Leck, P.J. Jansson, D.R. Richardson, Regulation of autophagy and apoptosis by Dp44mT-mediated activation of AMPK in pancreatic cancer cells, Biochim Biophys Acta 1866 (2020) 165657.

[33] D.S. Kalinowski, P.C. Sharpe, P.V. Bernhardt, D.R. Richardson, Design, synthesis, and characterization of new iron chelators with anti-proliferative activity: structure-activity relationships of novel thiohydrazone analogues, J. Med. Chem. 50 (2007) 6212-25.

[34] S. Sahni, K.C. Park, Z. Kovacevic, D.R. Richardson, Two mechanisms involving the autophagic and proteasomal pathways process the metastasis suppressor protein, N-myc downstream regulated gene 1, Biochim Biophys Acta 1865 (2019) 1361-1378.

[35] K.C. Park, S.V. Menezes, D.S. Kalinowski, S. Sahni, P.J. Jansson, Z. Kovacevic, D.R. Richardson, Identification of differential phosphorylation and sub-cellular localization of the metastasis suppressor, NDRG1, Biochim Biophys Acta 1864 (2018) 2644-2663.

[36] K.C. Park, B. Geleta, L.Y.W. Leck, J. Paluncic, S. Chiang, P.J. Jansson, Z. Kovacevic, D.R. Richardson, Thiosemicarbazones suppress expression of the c-Met oncogene by mechanisms involving lysosomal degradation and intracellular shedding, J. Biol. Chem. 295 (2020) 481-503.

[37] Z. Kovacevic, S. Chikhani, G.Y. Lui, S. Sivagurunathan, D.R. Richardson, The iron-regulated metastasis suppressor NDRG1 targets NEDD4L, PTEN, and SMAD4 and inhibits the PI3K and Ras signaling pathways, Antioxid. Redox Signal. 18 (2013) 874-87.

[38] R. Puertollano, S.M. Ferguson, J. Brugarolas, A. Ballabio, The complex relationship between TFEB transcription factor phosphorylation and subcellular localization, EMBO J. 37 (2018).

[39] A. Yamamoto, Y. Tagawa, T. Yoshimori, Y. Moriyama, R. Masaki, Y. Tashiro, Bafilomycin A1 prevents maturation of autophagic vacuoles by inhibiting fusion between autophagosomes and lysosomes in rat hepatoma cell line, H-4-II-E cells, Cell Struct. Funct. 23 (1998) 33-42.

[40] D.J. Klionsky, F.C. Abdalla, H. Abeliovich, R.T. Abraham, A. Acevedo-Arozena, K. Adeli, L. Agholme, M. Agnello, P. Agostinis, J.A. Aguirre-Ghiso, Guidelines for the use and interpretation of assays for monitoring autophagy, Autophagy 8 (2012) 445-544.

[41] S. Sahni, A.M. Merlot, S. Krishan, P.J. Jansson, D.R. Richardson, Gene of the month: BECN1, J. Clin. Pathol. 67 (2014) 656-60.

[42] F. Alessandrini, L. Pezzè, Y. Ciribilli, LAMPs: Shedding light on cancer biology, Semin. Oncol. 44 (2017) 239-253.

[43] J. Cárcel-Trullols, A.D. Kovács, D.A. Pearce, Cell biology of the NCL proteins: What they do and don't do, Biochim. Biophys. Acta 1852 (2015) 2242-55.

[44] Y. Liu, X. Xue, H. Zhang, X. Che, J. Luo, P. Wang, J. Xu, Z. Xing, L. Yuan, Y. Liu, X. Fu, D. Su, S. Sun, H. Zhang, C. Wu, J. Yang, Neuronal-targeted TFEB rescues dysfunction of the autophagy-lysosomal pathway and alleviates ischemic injury in permanent cerebral ischemia, Autophagy 15 (2019) 493-509.

[45] S. Yoshida, R. Pacitto, K. Inoki, J. Swanson, Macropinocytosis, mTORC1 and cellular growth control, Cell. Mol. Life Sci. 75 (2018) 1227-1239.

[46] D.R. Richardson, K. Milnes, The potential of iron chelators of the pyridoxal isonicotinoyl hydrazone class as effective antiproliferative agents II: the mechanism of action of ligands derived from salicylaldehyde benzoyl hydrazone and 2-hydroxy-1-naphthylaldehyde benzoyl hydrazone, Blood 89 (1997) 3025-38.

[47] I.J. Davis, B.L. Hsi, J.D. Arroyo, S.O. Vargas, Y.A. Yeh, G. Motyckova, P. Valencia, A.R. Perez-Atayde, P. Argani, M. Ladanyi, J.A. Fletcher, D.E. Fisher, Cloning of an Alpha-TFEB fusion in renal tumors harboring the t(6;11)(p21;q13) chromosome translocation, Proc. Natl. Acad. Sci. U. S. A. 100 (2003) 6051-6.

[48] R.P. Kuiper, M. Schepens, J. Thijssen, M. van Asseldonk, E. van den Berg, J. Bridge, E. Schuuring, E.F. Schoenmakers, A.G. van Kessel, Upregulation of the transcription factor TFEB in t(6;11)(p21;q13)-positive renal cell carcinomas due to promoter substitution, Hum. Mol. Genet. 12 (2003) 1661-9.

[49] R.M. Perera, S. Stoykova, B.N. Nicolay, K.N. Ross, J. Fitamant, M. Boukhali, J. Lengrand, V. Deshpande, M.K. Selig, C.R. Ferrone, J. Settleman, G. Stephanopoulos, N.J. Dyson, R. Zoncu, S. Ramaswamy, W. Haas, N. Bardeesy, Transcriptional control of autophagy-lysosome function drives pancreatic cancer metabolism, Nature 524 (2015) 361-5.

[50] A.E. Stacy, D. Palanimuthu, P.V. Bernhardt, D.S. Kalinowski, P.J. Jansson, D.R. Richardson, Structure-activity relationships of di-2-pyridylketone, 2-benzoylpyridine, and 2-acetylpyridine thiosemicarbazones for overcoming Pgp-mediated drug resistance, J. Med. Chem. 59 (2016) 8601-20.

Figure Legends

Figure 1. TFEB localization after incubation of cells with Dp44mT. (A) Line drawing of di-2-pyridylketone 4,4-dimethyl-3-thiosemicarbazone (Dp44mT). **(B)** PANC1 cells were incubated with control medium or this medium without FCS for 24 h/37°C. Cytoplasmic and nuclear fractions were then analyzed using western blot analysis to study the effect of these incubation conditions on the levels of TFEB, HDAC (nuclear control) and GAPDH (cytoplasmic control). **(C)** Densitometric analysis (arbitrary units) of the results in **(B)** for the 75 kDa TFEB band. **(D)** PANC1 cells were incubated with control medium or this medium containing Dp44mT (2.5- or 5-μM) for 24 h/37°C. Cytoplasmic and nuclear fractions were then analyzed using western blot analysis to study the effect of the experimental conditions on the expression of TFEB, HDAC and GAPDH. **(E)** Densitometric

analysis (arbitrary units) of the results in **(D)** for the 75 kDa TFEB band. Densitometry of bands was normalized to the corresponding β-actin standards. Results are shown as mean ± SEM (3 experiments): *$p < 0.05$, **$p < 0.01$; compared to the respective control cells. ##$p < 0.01$, ###$p < 0.001$; compared to the relative cytoplasmic treatment.

Figure 2. Dp44mT results in the nuclear translocation of TFEB. (A) PANC1 cells were incubated with control medium or this medium containing Dp44mT (1.25-, 2.5-, or 5-μM) for 24 h/37°C. Immunofluorescence analysis was then performed to study the co-localization of TFEB relative to DAPI-stained nuclei (DAPI, TFEB and Merge images; Scale bar: 22 μm; objective: 63x). The magnified image represents a 2.7-fold increase from that observed in the DAPI, TFEB and Merge images. Scale bar: 22 μm. Images are representative of three experiments. The quantification of intensity was performed with the intensity ratio nuclei cytoplasmic tool using ImageJ and represents the average intensity/cell with 24-30 cells being quantified/condition. **(B)** Quantitative analysis (arbitrary units) of TFEB intensity in **(A)**. Results are shown as mean ± SEM (3 experiments): *$p < 0.05$, ***$p < 0.001$; compared to control cells. #$p < 0.05$, ###$p < 0.001$; comparison of the nuclear and cytoplasmic fraction under the same conditions.

Figure 3. TFEB translocation to the nucleus is AMPK-dependent (A) PANC1 cells were pre-incubated for 48 h/37°C with either a negative control (NC) siRNA, or a selective siRNA against *AMPK*. Cells were then subsequently incubated with control medium or this medium containing Dp44mT (2.5 μM) for 24 h/37°C. Immunofluorescence analysis was then performed to study the co-localization of TFEB relative to DAPI-stained nuclei (DAPI, TFEB and Merge images; Scale bar: 22 μm; objective: 63x). The Magnified image represents a 2.7-fold increase from that observed in the DAPI, TFEB and Merge images. Scale bar: 22 μm. Images are representative of three experiments. The quantification of intensity was performed with the intensity ratio nuclei cytoplasmic tool using ImageJ and represents the average intensity/cell with 24-30 cells being quantified/condition. **(B)** Quantitative analysis (arbitrary units) of TFEB intensity in **(A)**. Results are shown as mean ± SEM (3 experiments): *$p < 0.05$ compared to the relative control cells. #$p < 0.05$, ##$p < 0.01$ comparison of nuclear and cytoplasmic fractions under the same condition.

Figure 4. *AMPK* silencing inhibits mTOR phosphorylation. (A) PANC1 cells were pre-incubated for 48 h/37°C with either a negative control (NC) siRNA, or a selective siRNA against *AMPK*. Cells were then subsequently incubated with control medium or this medium containing Dp44mT (2.5 μM) for 24 h/37°C. Western analysis was then performed to study the effect on the levels of total AMPK, p-AMPK (Thr172), p-TSC2 (Ser1387), TSC2, p-mTOR (Ser2448), mTOR and β-actin. **(B)** Densitometric analysis (arbitrary units) of the results in **(A)**. Results are shown as mean ± SEM (3 experiments). Densitometry of bands was normalized to the corresponding β-actin standards.

*$p < 0.05$, **$p < 0.01$, ***$p < 0.001$; compared to control cells. #$p < 0.05$, ##$p < 0.01$; compared to relative control treatment; †$p < 0.05$ comparison of the activity of Dp44mT (2.5 μM) between the NC siRNA and AMPK siRNA-treatment.

Figure 5. Dp44mT increases LC3-II expression in a TFEB-dependent manner. (A) PANC1 cells were pre-incubated for 48 h/37°C with either NC siRNA or *TFEB* siRNA. The cells were then subsequently incubated with control medium or this medium containing Baf A1 (100 nM) for 30 min/37°C followed by either control medium or this medium containing Dp44mT (2.5 μM) for 24 h/37°C. Western blot analysis was then performed to study the effect of these experimental conditions on the levels of LC3-I, LC3-II, TFEB, or β-actin. **(B)** Densitometric analysis (arbitrary units) of the results in **(A)**. **(C)** PANC1 cells were pre-incubated for 48 h/37°C with either NC siRNA or *TFEB* siRNA. Cells were then subsequently incubated with control medium or this medium containing Dp44mT (2.5 μM) for 24 h/37°C. Western blot analysis was then performed to study the effect of these experimental conditions on total TFEB or Beclin-1 levels. **(D)** Densitometric analysis (arbitrary units) of the results in **(C)**. Densitometry of bands was normalized to the corresponding β-actin standards. Results are shown as mean ± SEM (3 experiments). *$p < 0.05$, ***$p < 0.001$ compared to the relative NC siRNA control cells. #$p < 0.05$, ##$p < 0.01$; compared to the respective treatment without Baf A1. † $p < 0.05$, †† $p < 0.01$; compared to respective control treatment, or as indicated. ~ $p < 0.05$ compared to respective Dp44mT-treated NC siRNA condition.

Figure 6. Effect of *AMPK* or *TFEB* silencing on the expression of the lysosomal markers, lysosomal-associated membrane protein 2 (LAMP2) and cathepsin D. (A) PANC1 cells were pre-incubated for 48 h/37°C with either NC siRNA, or *TFEB* siRNA. Cells were then subsequently incubated with control medium or this medium containing Dp44mT (2.5 μM) for 24 h/37°C. Western blot analysis was then performed to study the effect on AMPK, LAMP2, cathepsin D, or β-actin levels. **(B)** Densitometric analysis (arbitrary units) of the results in **(A)**. **(C)** PANC1 cells were pre-incubated for 48 h/37°C with either NC siRNA or *TFEB* siRNA. Cells were then subsequently incubated with control medium or this medium containing Dp44mT (2.5 μM) for 24 h/37°C. Western blot analysis was then performed to study the effect on TFEB, LAMP 2, cathepsin-D, or β-actin expression. **(D)** Densitometric analysis (arbitrary units) of the results in **(C)**. Densitometry of bands was normalized to the corresponding β-actin standards. Results are shown as mean ± SEM (3 experiments). *$p < 0.05$, **$p < 0.01$; ***$p < 0.001$ compared to relative NC siRNA control cells. #$p < 0.05$ compared to the respective control treatment, or as shown.

Figure 7. Schematic overview of the effect of Dp44mT on the TFEB regulation. The chelator, Dp44mT, induces translocation of TFEB to the nucleus through two processes. Once activated, AMPK inhibits mTORC1, by inhibiting the phosphorylation of mTOR. Dp44mT also inhibits mTORC1 by preventing complex formation by phosphorylation of raptor by an AMPK-dependent mechanism. The inhibition of mTORC1 results in dephosphorylation of TFEB, allowing it to be translocated to the nucleus. This activation of TFEB leads to increased autophagic initiation. However, Dp44mT induces lysosomal membrane permeabilization (LMP), resulting in dysfunctional autophagy [14].

Declaration of competing interests

☒ The authors declare that they have no known competing financial interests or personal relationships that could have appeared to influence the work reported in this paper.
☐The authors declare the following financial interests/personal relationships which may be considered as potential competing interests:

Credit Author Statement

Des R. Richardson: Initial Idea, Conceptualization, Writing, Draft Preparation; Editing and Reviewing; Acquisition of Funding

Sumit Sahni: Conceptualization, Writing, Draft Preparation; Reviewing and Editing; Acquisition of Funding; Experimental

Sukriti Krishan: Writing, Draft Preparation; Experimental; Reviewing and Editing

Highlights

Dp44mT shows potent anti-cancer activity through its ability to target lysosomes
Dp44mT induces nuclear translocation of the major regulator of autophagy, TFEB
Dp44mT-mediated nuclear translocation of TFEB was AMPK-dependent
Dp44mT regulates TFEB translocation through AMPK activation and mTORC1 inhibition
AMPK activation by Dp44mT plays a role in lysosomal biogenesis and TFEB function

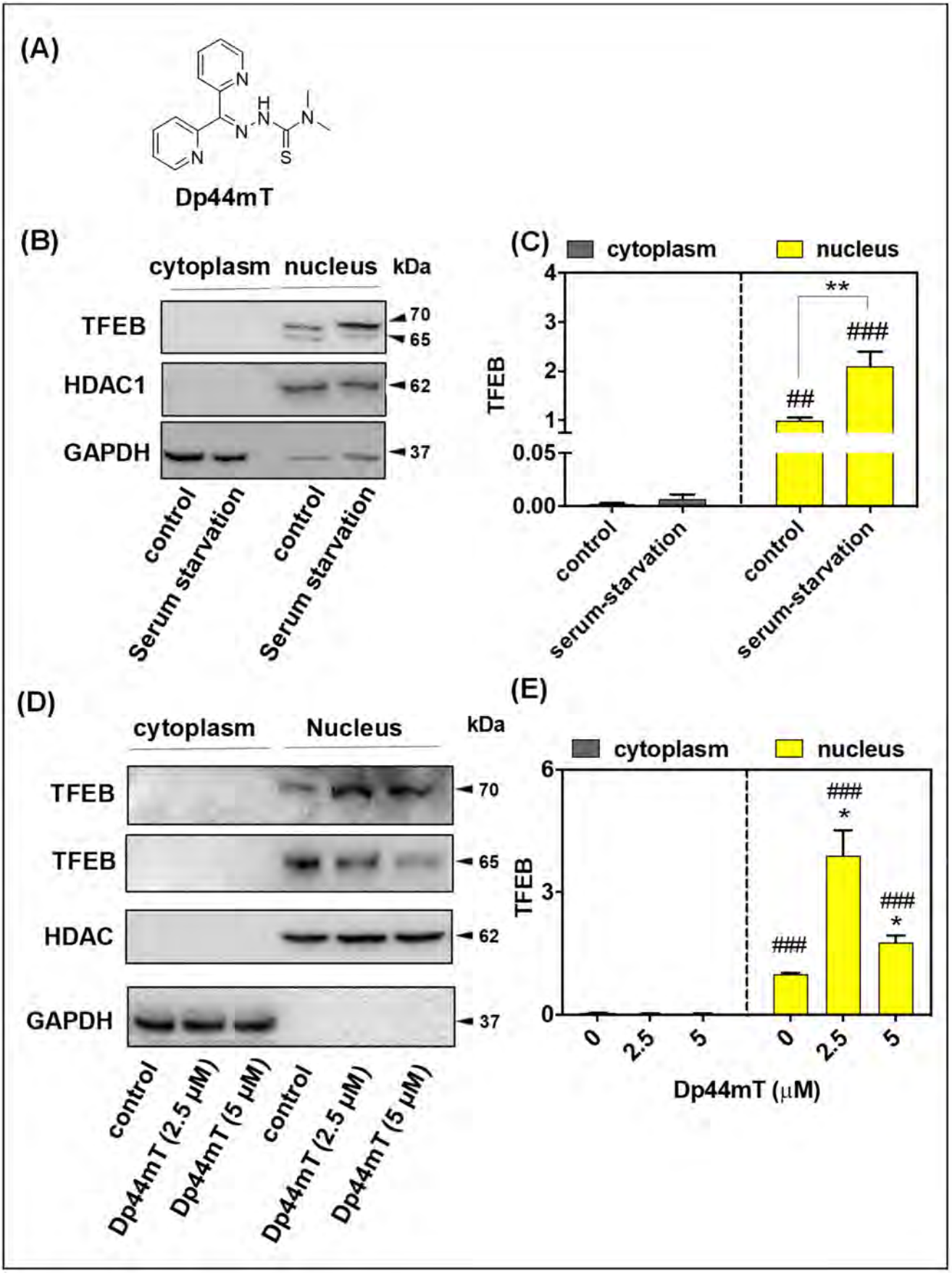
(A)
Dp44mT
(B)
cytoplasm
nucleus
kDa
TFEB
HDAC1
GAPDH
70
65
62
37
control
Serum starvation
control
Serum starvation
(C)
cytoplasm
nucleus
TFEB
**
###
##
control
serum-starvation
control
serum-starvation
(D)
cytoplasm
Nucleus
kDa
TFEB
TFEB
HDAC
GAPDH
70
65
62
37
control
Dp44mT (2.5 μM)
Dp44mT (5 μM)
control
Dp44mT (2.5 μM)
Dp44mT (5 μM)
(E)
cytoplasm
nucleus
TFEB
###
*
###
*
###
Dp44mT (μM)

Figure 1

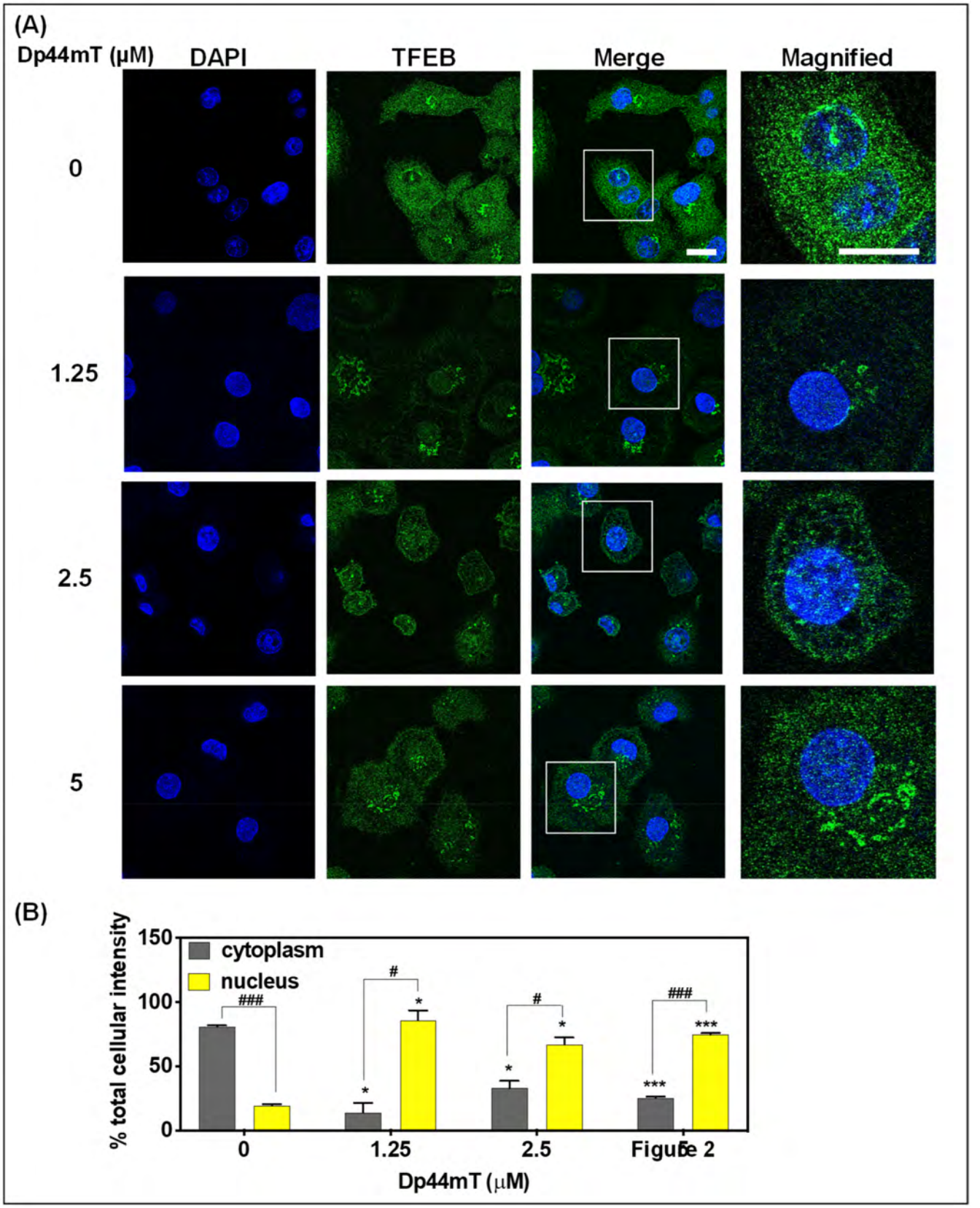
(A)
Dp44mT (μM)
DAPI
TFEB
Merge
Magnified
0
1.25
2.5
5
(B)
% total cellular intensity
150
100
50
0
cytoplasm
nucleus
###
#
*
***
0
1.25
2.5
5
Dp44mT (μM)

Figure 2

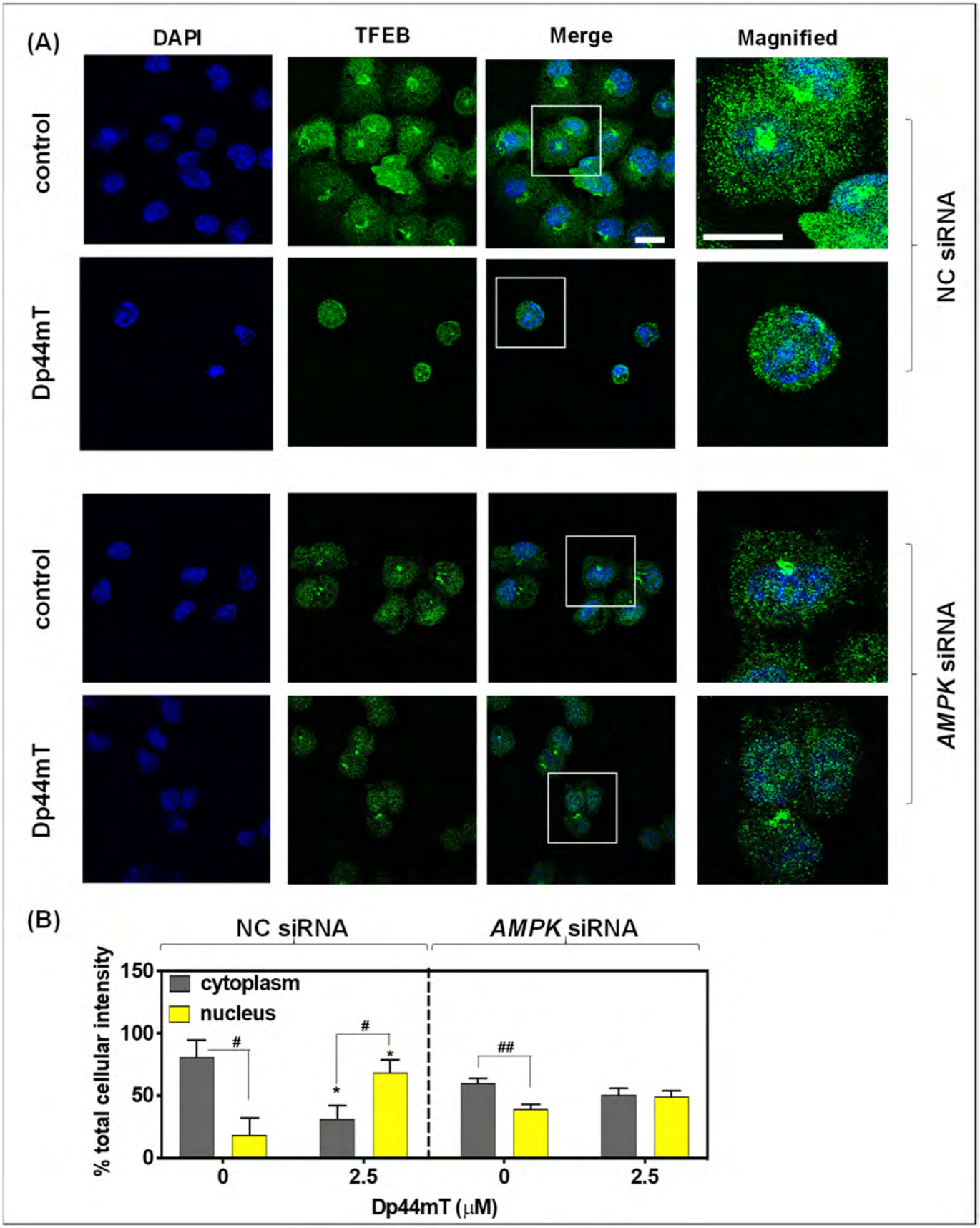
(A)
DAPI
TFEB
Merge
Magnified
control
Dp44mT
NC siRNA
control
Dp44mT
AMPK siRNA
(B)
NC siRNA
AMPK siRNA
% total cellular intensity
150
100
50
0
cytoplasm
nucleus
#
#
*
*
##
0
2.5
0
2.5
Dp44mT (μM)

Figure 3

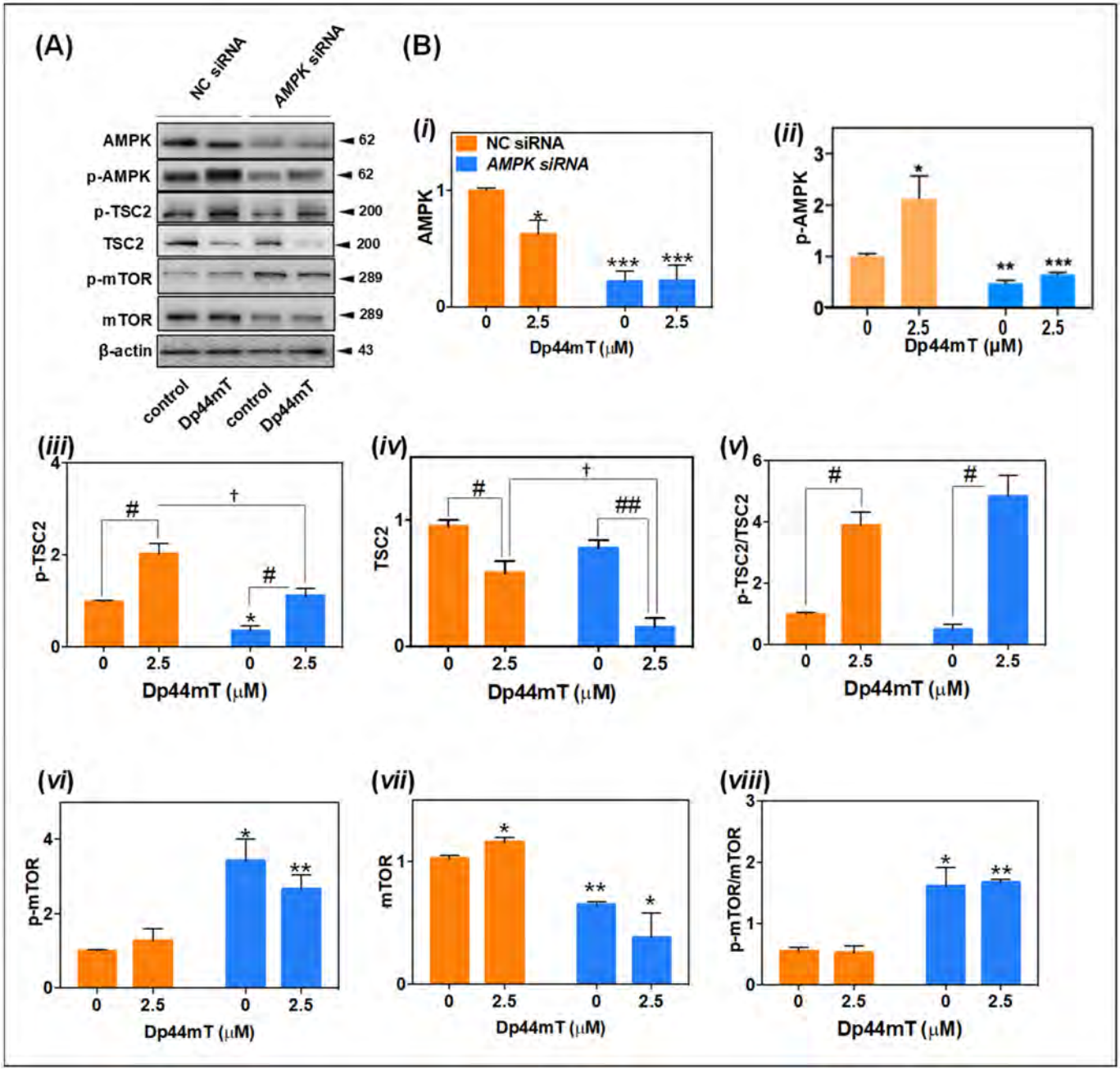
(A)
NC siRNA
AMPK siRNA
AMPK
p-AMPK
p-TSC2
TSC2
p-mTOR
mTOR
β-actin
62
62
200
200
289
289
43
control
Dp44mT
control
Dp44mT
(B)
(i)
NC siRNA
AMPK siRNA
AMPK
Dp44mT (μM)
(ii)
p-AMPK
Dp44mT (μM)
(iii)
p-TSC2
Dp44mT (μM)
(iv)
TSC2
Dp44mT (μM)
(v)
p-TSC2/TSC2
Dp44mT (μM)
(vi)
p-mTOR
Dp44mT (μM)
(vii)
mTOR
Dp44mT (μM)
(viii)
p-mTOR/mTOR
Dp44mT (μM)

Figure 4

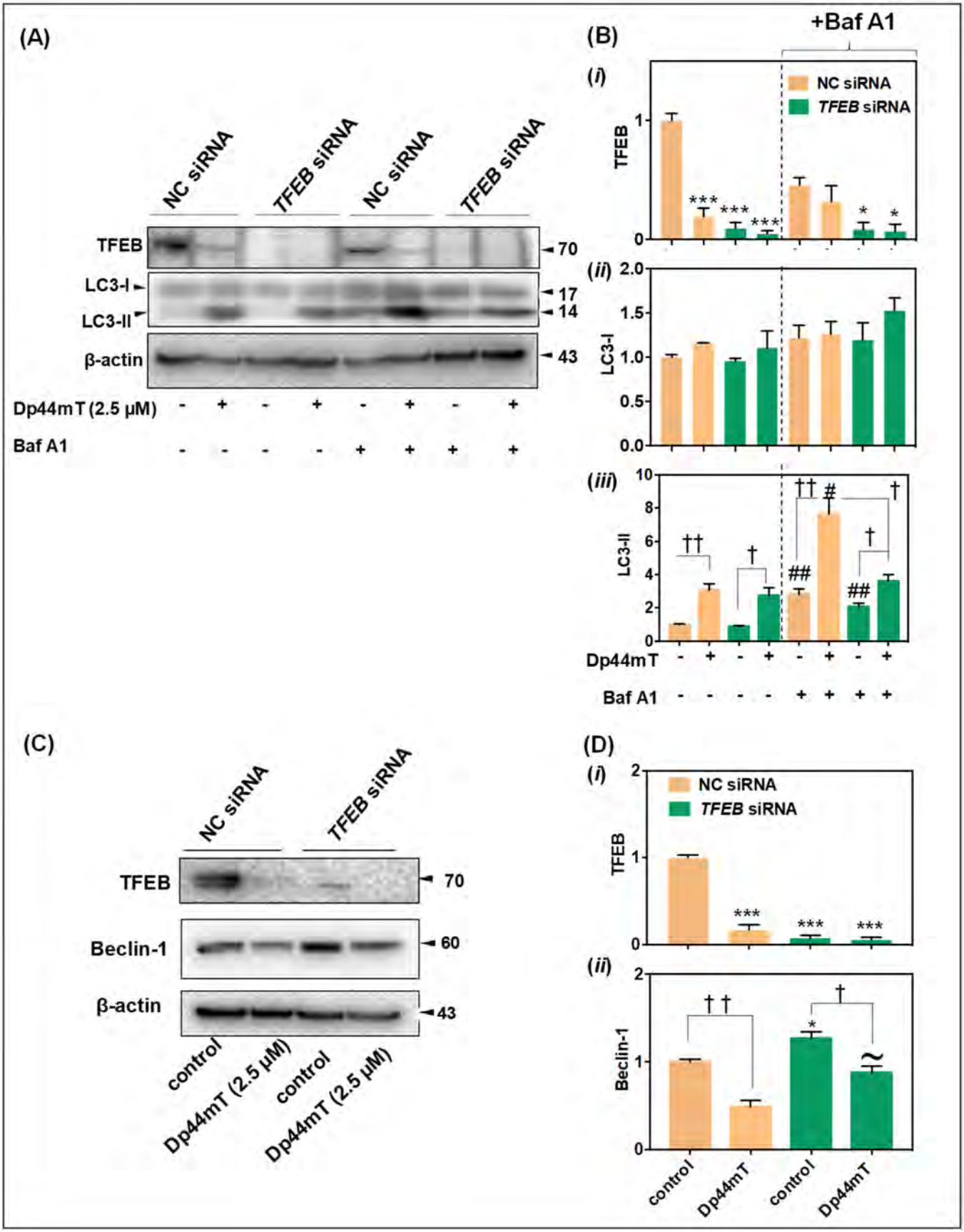
(A)
NC siRNA
TFEB siRNA
NC siRNA
TFEB siRNA
TFEB
LC3-I
LC3-II
β-actin
70
17
14
43
Dp44mT (2.5 μM)
Baf A1
(B)
+Baf A1
(i)
NC siRNA
TFEB siRNA
TFEB
(ii)
LC3-I
(iii)
LC3-II
Dp44mT
Baf A1
(C)
NC siRNA
TFEB siRNA
TFEB
Beclin-1
β-actin
70
60
43
control
Dp44mT (2.5 μM)
control
Dp44mT (2.5 μM)
(D)
(i)
NC siRNA
TFEB siRNA
TFEB
(ii)
Beclin-1
control
Dp44mT
control
Dp44mT

Figure 5

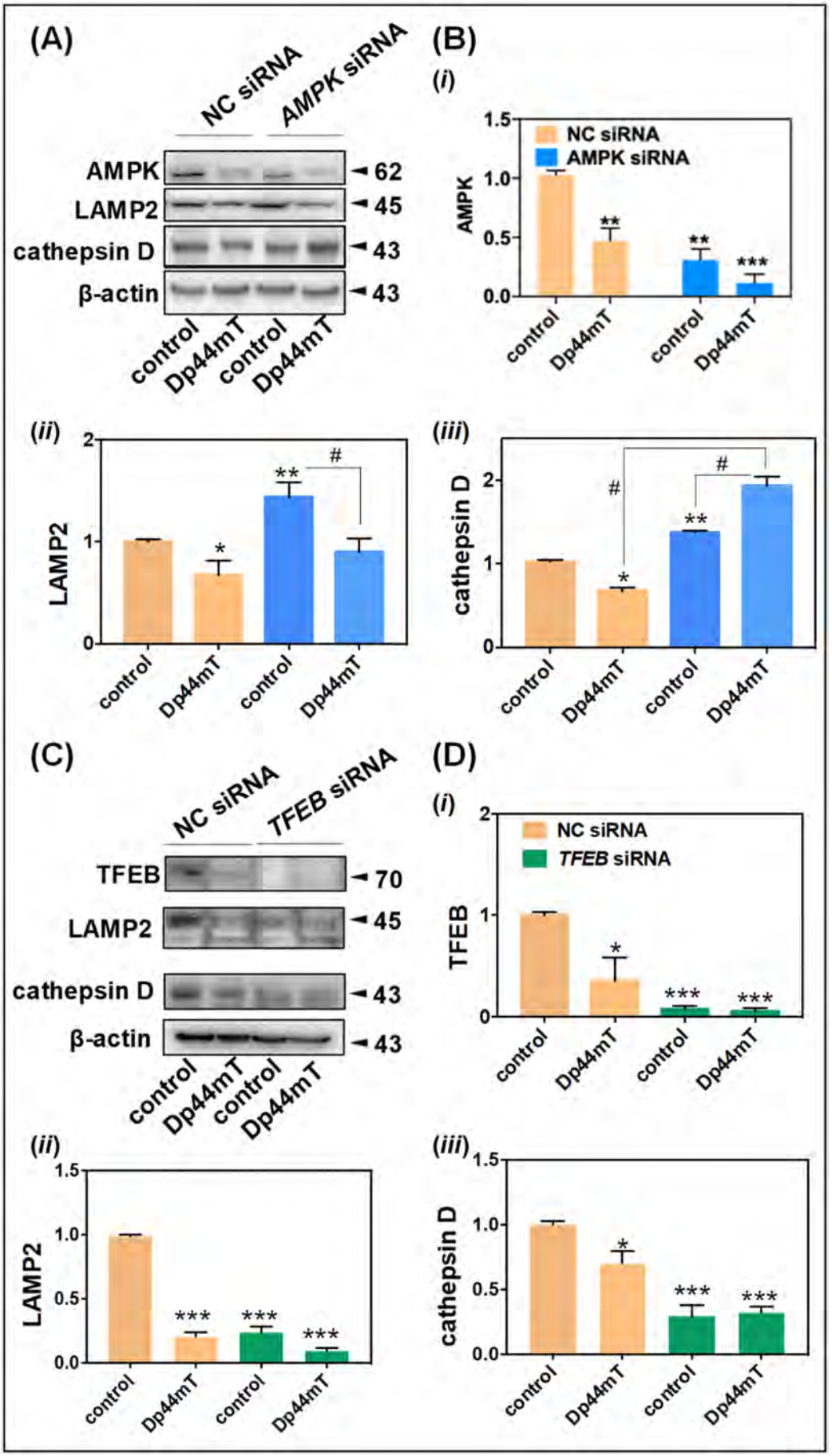
(A)
NC siRNA
AMPK siRNA
AMPK
LAMP2
cathepsin D
β-actin
62
45
43
43
control
Dp44mT
control
Dp44mT
(B)
(i)
NC siRNA
AMPK siRNA
AMPK
1.5
1.0
0.5
0.0
**
**
***
control
Dp44mT
control
Dp44mT
(ii)
LAMP2
2
1
0
*
**
#
control
Dp44mT
control
Dp44mT
(iii)
cathepsin D
2
1
0
#
#
*
**
control
Dp44mT
control
Dp44mT
(C)
NC siRNA
TFEB siRNA
TFEB
LAMP2
cathepsin D
β-actin
70
45
43
43
control
Dp44mT
control
Dp44mT
(D)
(i)
NC siRNA
TFEB siRNA
TFEB
2
1
0
*
***
***
control
Dp44mT
control
Dp44mT
(ii)
LAMP2
1.5
1.0
0.5
0.0
***
***
***
control
Dp44mT
control
Dp44mT
(iii)
cathepsin D
1.5
1.0
0.5
0.0
*
***
***
control
Dp44mT
control
Dp44mT

Figure 6

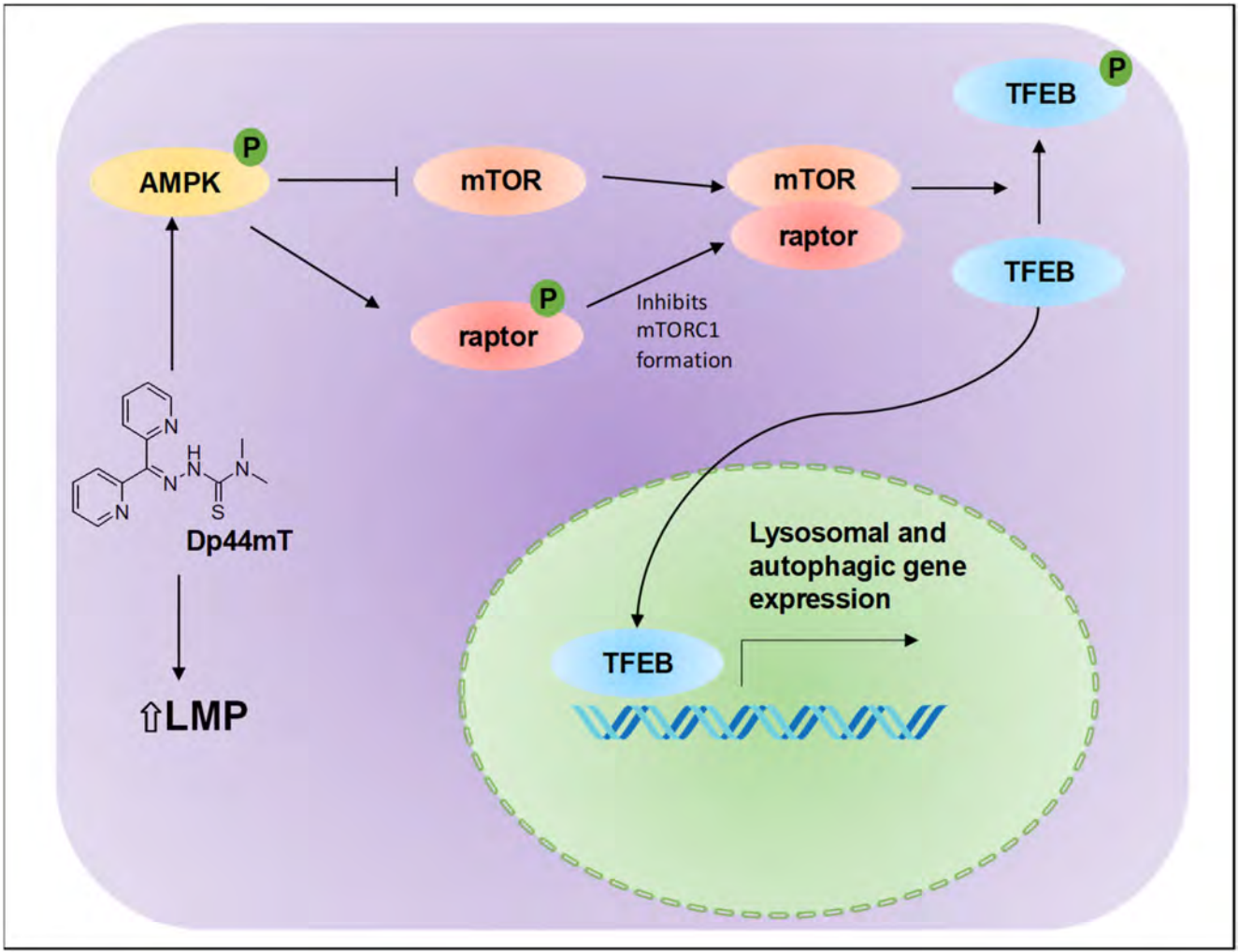
TFEB
P
AMPK
P
mTOR
mTOR
raptor
TFEB
raptor
P
Inhibits
mTORC1
formation
Dp44mT
⇧LMP
Lysosomal and
autophagic gene
expression
TFEB

Figure 7